



Design and Enactment Evaluation of Adaptive Artifacts Removal from EEG Signal Records

Ramu Kaliya Perumal^{1*}, S.V.S. Rama Krishnam Raju², Amit Kumar Chandanan³, Dasari Manasa⁴,
Rajeev Pandey⁵, Modugu Dileep Kumar⁶, Neerugatti Varipallay Vishwanath⁷, Tanuja Kashyap⁸

¹ Department of Computer Science Engineering, Aarupadai Veedu Institute of Technology (AVIT), Vinayaka Mission's Research Foundation, Paiyanoor, Chennai 603104, India

² Department of Electronics and Communication Engineering, Dean Academic, St. Martin's Engineering College, Secunderabad 500100, India

³ Department of CSIT, Guru Ghasidas Vishwavidyalay, Bilaspur (C.G.) 495009, India

⁴ Department of Computer Science Engineering, Koneru Lakshmaiah Education Foundation, Vaddeswaram 522302, India

⁵ Department of Computer Science Engineering, University Institute of Technology, RGPV, Bhopal 462033, India

⁶ Department of Computer Science Engineering, St Martin's Engineering College, Secunderabad 500100, India

⁷ Department of Electronics and Communication Engineering, St. Martin's Engineering College, Secunderabad, Telangana 500100, India

⁸ Department of Electronics and Telecommunication Engineering, Bhilai Institute of Technology Durg, Chhattisgarh 491001, India

Corresponding Author Email: k.ramu147@gmail.com

Copyright: ©2024 The authors. This article is published by IETA and is licensed under the CC BY 4.0 license (<http://creativecommons.org/licenses/by/4.0/>).

<https://doi.org/10.18280/ria.380429>

ABSTRACT

Received: 28 August 2023

Revised: 1 February 2024

Accepted: 12 March 2024

Available online: 23 August 2024

Keywords:

EEG, NN, PCA, ICA, FLM

Various factors, such as electrical power lines, EOG or ECG interference, contribute to artefacts in Electroencephalogram (EEG) data, complicating EEG analysis and clinical interpretation. Developing specialized filters to mitigate these artefacts is crucial. Artefacts from eye movements and blinks have been extensively studied, prompting the development of an FLM optimization-based learning technique for a Neural Network (NN)-enhanced adaptive filtering model to address them. Initially, Firefly (FF) and LM adaptive filter algorithms analyze EEG data to determine optimal weights. These weights are then incorporated into the NN for adaptive filtering. The resulting technique effectively eliminates artefacts. Performance evaluation, based on Signal to Noise Ratio (SNR), Root Mean Square Error (RMSE), Mean Square Error (MSE), and computing time, compares the proposed method with conventional approaches. Results demonstrate a significant 92% improvement in SNR, indicating the efficiency of the proposed technique. This advancement holds promise for enhancing EEG data quality and facilitating more accurate clinical assessments.

1. INTRODUCTION

One or more factors may be involved in the transmission of a signal. For a structure to be considered in acceptable condition or performance, it must be able to accurately record and provide information about a living structure, and then the signal is referred to as biological. When a CT scan is used, the X-ray absorption patterns can be used to create a spatial pattern, and a scalp electrode can be used to generate voltage. As a medical or biological source transmits, the biomedical signal [1] is considered to be a biomedical signal [2]. Waves in biomedical signals have been observed in a variety of physiological activities, tissues, and organs, ranging from gene and protein sequences to cardiac and brain rhythms [3].

Biological signals present a blend of signal and noise, necessitating careful observation. Noise, stemming from various sources such as equipment (sensors, amplifiers, filters), or unrelated asynchronous signals, can obscure valuable data [4]. Medical signal processing emerges as a vital technology

aimed at extracting meaningful insights from biological signals. Employed by biologists and medical professionals alike, biomedical signal processing facilitates the exploration of novel biological phenomena and the identification of specific disorders. Central to this process is the accurate quantification of the signal model and its components, alongside the essential task of noise removal. Through meticulous signal processing, the objective is to delineate the underlying signal from the interfering noise, thereby enabling clearer interpretation and analysis of biological data. In Biological signal processing [5], the primary goal is to reduce background noise. Noise can be generated because of the interference between instruments and electrical lines. Subsystems that interact with the body in complex systems are also contained inside a biological subsystem. recordings; however, the process fails to entirely separate the ocular artefacts from the EEG signal, particularly when the amplitudes are similar. As a result, this study contributes to the development of new methods [6].

A new wavelet-based technique. W-ICA, which shows the wavelet scheme's performance capability, makes it easier to remove artefacts through the use of Haar wavelet with an ICA model. Experiments showed that the intended work is better than it was previously thought to be [7].

There are a variety of variables that limit the diagnostic procedure, including the inability to detect specific characteristics in signals and the limitations of human extraction skill. This manual analysis also suffers from human faults. These mistakes occur as a result of the decision-making process being weakened by weariness and subjectivity [8-10].

First, sensors are used to identify the physical characteristics of the biomedical system. An ECG signal, for example, measures the electrical activity of cardiac muscles and is used to determine the heart's functioning qualities. Filtering and pre-processing are the next steps. After the sensor has recorded the biological signal, this must be done. There may be unwanted noise in the biological signal, thus pre-processing and filtering are necessary. For example, the electrical impulses produced by the respiratory system are the primary source of ECG signal interference and noise [11].

2. EXISTING WORK DONE

This section evaluates the standard methods currently in use to clean up EEG data. An innovative BSS approach, IVA, was implemented by researchers to simultaneously employ HOS and SOS to remove OA and muscle motion artefacts. The efficiency of the IVA system was also studied by using both the simulated results and the components to read EEG data. Integration of IVA to combine HOS and SOS processes into a single step shows superior results in isolating OA and muscle action artefacts, especially for raw EEG with a low signal-to-noise ratio (SNR) [12]. The issues with EED artefacts eradication have been resolved thanks to a reliable, automated, and resilient technique established in the study [13, 14]. The suggested method relied on the Haar function and utilised straightforward threshold-based artefacts removal and wavelet domain denoising methods. So, the results of the hardware's execution were made available as well. Nine in-depth case studies using both synthetic and actual data have been developed and evaluated after extensive database analysis. At last, the established method was detailed, and its validity was proven using an FPGA platform.

The authors devised a novel hybrid model, combining Active Noise Control (ANC) and Independent Component Analysis (ICA) [15]. This innovative approach utilized ICA to pre-process EEG signals, eliminating artefacts before applying NN-based ANC. Remarkably, the method achieved artefact reduction without requiring additional electrodes, using only a limited number of EEG signals. It demonstrated efficacy in reducing artefacts with minimal latency, rendering it suitable for real-time Brain-Computer Interface (BCI) applications. Evaluation involved cue-dependent BCI data to ensure consistent performance. Comparative analysis against standard schemes, conducted through online and offline simulations [16-18], revealed superior artefact removal and restoration of essential EEG signals by the proposed method. These findings underscore the efficacy and potential of the hybrid strategy in enhancing signal quality for BCI systems.

To eliminate distracting EEG noise, researchers [19-21] suggest utilising a FLM learning strategy in conjunction with a neural network (NN) based method. At first, the EEG input

was provided to AF so that LM and FF could calculate ideal weights. NN was trained with a hybrid of the two approaches, and the resulting AF weights were used effectively. Finally, the model-based AF method is superior at eliminating artefacts in EEG data. Finally, the SNR, computing time, RMSE, and MSE behaviours of the recommended model and the baseline models were compared and contrasted. The results show that the SNR is significantly improved by the method used, by 42.042 dB [22, 23].

3. PROPOSED ALGORITHM

Electroencephalography (EEG) is a method used in neurophysiology for measuring brain electrical activity through the use of electrodes attached to the scalp. These aberrations are a result of the mingling of EEG data with other physiological signals. Electrical cardiograms, Electro-oculogram, and electromyograms are all examples of such artefacts.

The medical field faces significant challenges in eliminating artefacts from EEG data, prompting the development of innovative solutions. This study introduces a learning algorithm based on FLM optimization for NN-enhanced adaptive filtering, aimed at mitigating artefacts effectively.

Initially, the adaptive filter is employed on the EEG signal to determine optimal weights using two renowned optimization methods: the Firefly (FF) algorithm and the Levenberg-Marquardt (LM) algorithm. These methods converge at the neural network (NN), which plays a pivotal role in achieving adaptive filtering by computing appropriate weights. Consequently, the proposed filtering approach enhances artefact removal capabilities.

Subsequently, the model's performance is evaluated using metrics like Signal-to-Noise Ratio (SNR), Mean Square Error (MSE), and Root Mean Square Error (RMSE) following adjustments to hidden neurons. These evaluations provide insight into the efficacy of the developed model in artefact reduction and signal enhancement.

By integrating FLM optimization with NN-enhanced adaptive filtering, this study offers a promising framework for addressing artefacts in EEG data. The utilization of established optimization algorithms coupled with neural network architecture showcases a robust methodology for improving EEG data quality and clinical interpretation.

It is generally accepted that adaptive noise cancellation can help get rid of artefacts. The fundamental schematic depicting the realisation of adaptive noise cancellation is shown in Figure 1. More so, we get our first data from the input source $S(t)$. After that, we get the subsequent input from the source denoted by $A(t)$. Here, the noise at issue pinpoints the place where EMG, EOG, and ECG artefacts first emerge. The interference signal $I(t)$ is generated when the noisy source signal of the artefacts signal is "acquiesced" by unanticipated non-linear dynamics. Then, the clear signal adds to the interference signal to create the primary input signal, represented as follows:

$$p(t) = s(t) + I(t) \quad (1)$$

The signal at the input, denoted as $S(t)$, and the signal at the output, denoted as $I(t)$, are the two terms in Eq. (1). Subsequently, adaptive filtering is applied to the signal generated by the noise source in order to obtain the filtered

output. The interference signal, which is the result of nonlinear dynamics, is remarkably similar to the output of the producing filter. Retrieving clean EEG data is the primary focus of noise cancellation. In addition, the filtered response is reduced relative to the original input (specified by Eq.) in order to retrieve the clean EEG data (2).

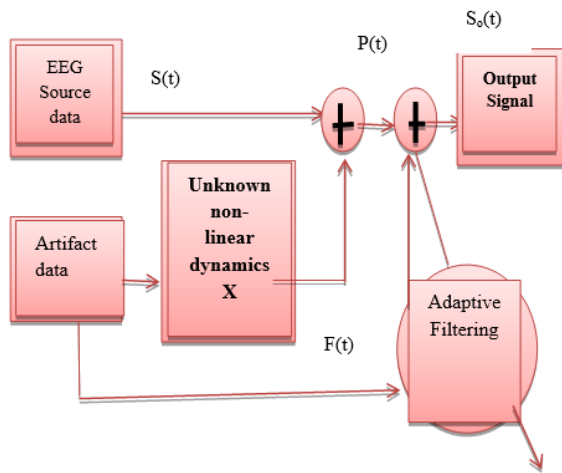


Figure 1. The proposed algorithm

$$S_o(t) = S(t) + I(t) - F(t) \quad (2)$$

When analysing the model in terms of time series prediction, the NARX model works exceptionally well. Typically, a time series' reaction is predicated on a signal whose values are sequentially correlated with both the input signal and the preceding data. The method is called NARX if and only if the input to the system can be uniquely identified as a computable quantity. NARX uses a three-vector-layer structure, with the hidden layer serving as the input and the output layer serving as the final layer.

Here, we have an input vector, a delayed output vector, and another input vector all making up the input layer of our data structure (delayed). After NN is applied, the resultant vector is $L(n+1)$.

$$L(n+1) = f(L(n), \dots, L(n-D_L); V(n), \dots, V(n-D_V)) \quad (3)$$

It was the input vector $L(n)$ that was being referred to in Eq. (3). The delayed values of the regressed output vector are then represented by the notation $L(n-1), L(n-2), \dots, L(n-D_L)$. $V(n), V(n-1), V(n-D_V)$ is then the representation of the delayed input vector's sequence. The NARX-NN procedure begins with the assignment of weights between the hidden units and the input vector and between the hidden units and the regressed output vector.

In order to improve optimization performance, this model employs a hybrid method based on a combination of the FF algorithm and the LM algorithm. While attempting to implement the NARX-NN method, the FF approach is initially considered. As such, the blinking habits of the FF are necessary for the FF algorithm. In the FF model, the feasible solution vector is calculated from the coordinates of each FF. Brightness changes the position of FF. Any FF that can't pin down the source of the brightness just picks a number and moves it. Here, the brightness value is determined by the solution to an optimization problem. FF's unpredictable motion increases processing cost and slows down solution

convergence. As a result, the firefly method produces non-feasible solutions and has a slower convergence rate.

This study employs the LM algorithm alongside the FF algorithm to resolve the problems associated with the convergence of the optimization concept. This is how the object's location is determined, which is necessary for reconciling theoretical and experimental results. In addition, the LM procedure collaborates with the Gauss-Newton model to function on the steepest descent clustering. The learning process is efficient and quick in the model as well. As a result, the hybrid learning method proved to be more effective in rapidly training the model.

Figure 2 depicts the NARX NN model, employing a learning technique to integrate three distinct weights: exogenous input, regressed result, and exogenous/regressed output. Initially, the LM and learning algorithm receive a randomly generated input vector. Once the optimization principle is finalized, both LM and FF learning models produce weight vectors. This approach ensures comprehensive incorporation of input factors, enhancing the model's adaptability and performance. The vectors are as follows:

$$W^{LM} = W^{L1} + W^{L2} + W^{L3} + \dots + W^{Lk} \quad (4)$$

$$W^{ff} = W^{f1} + W^{f2} + W^{f3} + \dots + W^{fk} \quad (5)$$

The following steps are used for atomised EEG artifact detection and removal:

- 1) The population size is determined (along dimension). Additionally, both the beauty and intensity factors are initialised with made-up values. Finally, the weight vector is used to seed the random FF.
- 2) The entails developing the fitness function.
- 3) Compare different FFs based on their brightness levels. Every FF's location is updated based on the luminosity of its nearest neighbouring FF.
- 4) Determine the intensity, attractiveness, and fitness values.

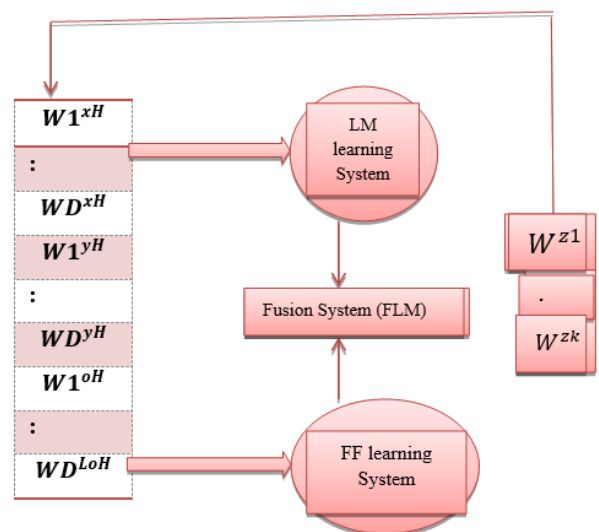


Figure 2. The proposed Hybrid NARX-NN scheme

- 5) The global solution or the best solution at the moment is determined by ranking fireflies.
- 6) Keep this pattern going till the maximum number of iterations is reached.
- 7) Formulate the value of error among the current value and the expected value.

8) The LM model is then used to initialise the weight vector in the NARX NN based on the magnitude of the hidden weights.

9) Calculate the sum squared error.

10) The LM algorithm equation is used to update the input weights.

11) If there is a minimal trail-weighted function rather performance index to update the weight according to the equation below.

12) Measuring the Learning Rate at a time when the Performance Index is lower than the Trail Function.

13) The LM formula is used to adjust the previously arbitrary weight.

14) Generate the gradient matrix from the Jacobian matrix.

15) The outcome of the LM method is represented by using the weights from the input vector and the updated weights.

16) The LM algorithm, an error value is calculated by subtracting the error from the ground truth value and applying the new weight.

17) The results from the FF model and the LM model are used to generate the final weight vector. The examination of the error value of the LM and FF model is important for moving forward with the optimization process. The LM algorithm's output is only relevant to the weight vector if its error value is smaller than the FF algorithm's error value ($ELM < EFF$).

Concurrently, the weight vector is selected from the FF algorithm's output if its error value is smaller than the LM algorithm's error value ($ELM > EFF$). When this happens, the current error value is less than the previous error value ($E_{t+1} < E_t$), and the damping factor value is at its lowest. When the current error is larger than the previous error ($E_t > E_{t+1}$), the damping factor is increased. Last but not least, the FLM learning algorithm's error value comparison yields the weight vector.

A. The database applied:

The authentic signal used in this study came from the Physionet database. Additionally, we conducted an analysis of the proposed method's efficiency. Various artefacts, including Electromyographic (EMG), Electrooculogram (EOG), and

Electrocardiographic (ECG), were introduced into a genuine signal to show the presented method. Real-time applications were used to test the created model, which was then implemented in MATLAB. The CHB-MIT scalp EEG database is used as the input database. In this case, each of the first five signals downloaded lasted one minute.

4. RESULT AND DISCUSSION

The three types of ECG, EMG, and EOG artefacts signals present in the input EEG signals are shown in Figures 3, 4 and 5, respectively (where x-axis is time in ms and y-axis is amplitude in μV).

In Figure 3, x-axis is time in ms and y-axis is amplitude in μV . The EEG signal is added with selected ECG artifact. Therefore, produced artifact added signal. This artifact added or artifactual signal is filter with the proposed NARX NN method and results are presented. The visual interpretation suggested that the proposed method is effective for removing ECG artifact successfully and filtered output is very close to the pure EEG signal, proves the success of the proposed algorithm.

In Figure 4, x-axis is time in ms and y-axis is amplitude in μV . The EEG signal is added with selected EMG artifact. Therefore, produced artifact added signal. This artifact added or artifactual signal is filter with the proposed NARX NN method and results are presented. The visual interpretation suggested that the proposed method is effective for removing EMG artifact successfully and filtered output is very close to the pure EEG signal, proves the success of the proposed algorithm.

In Figure 5, x-axis is time in ms and y-axis is amplitude in μV . The EEG signal is added with selected ECG artifact. Therefore, produced artifact added signal. This artifact added or artifactual signal is filter with the proposed NARX NN method and results are presented. The visual interpretation suggested that the proposed method is effective for removing EOG artifact successfully and filtered output is very close to the pure EEG signal, proves the success of the proposed algorithm.

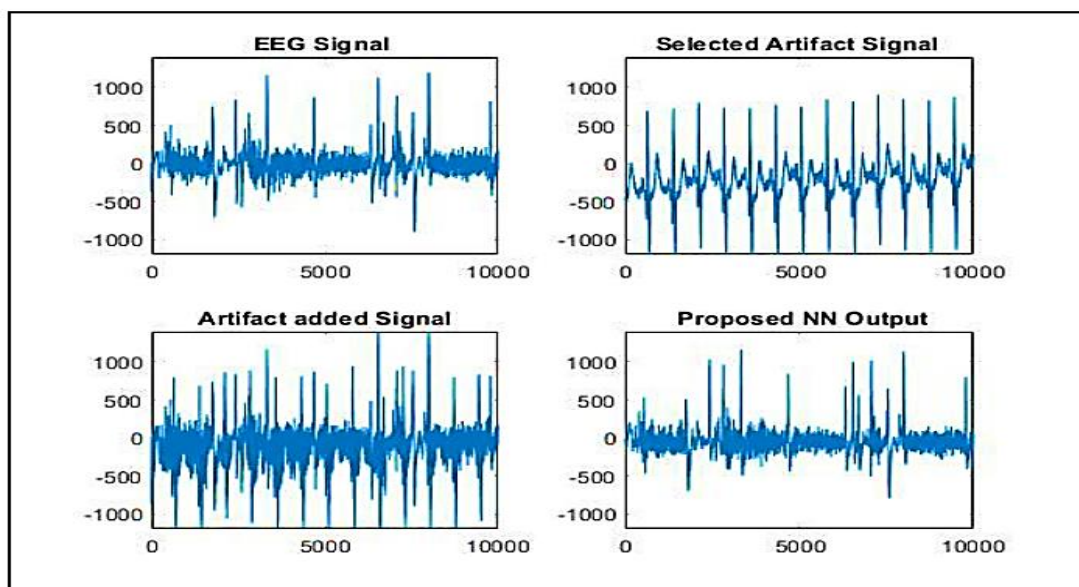


Figure 3. EEG signal with ECG artifact

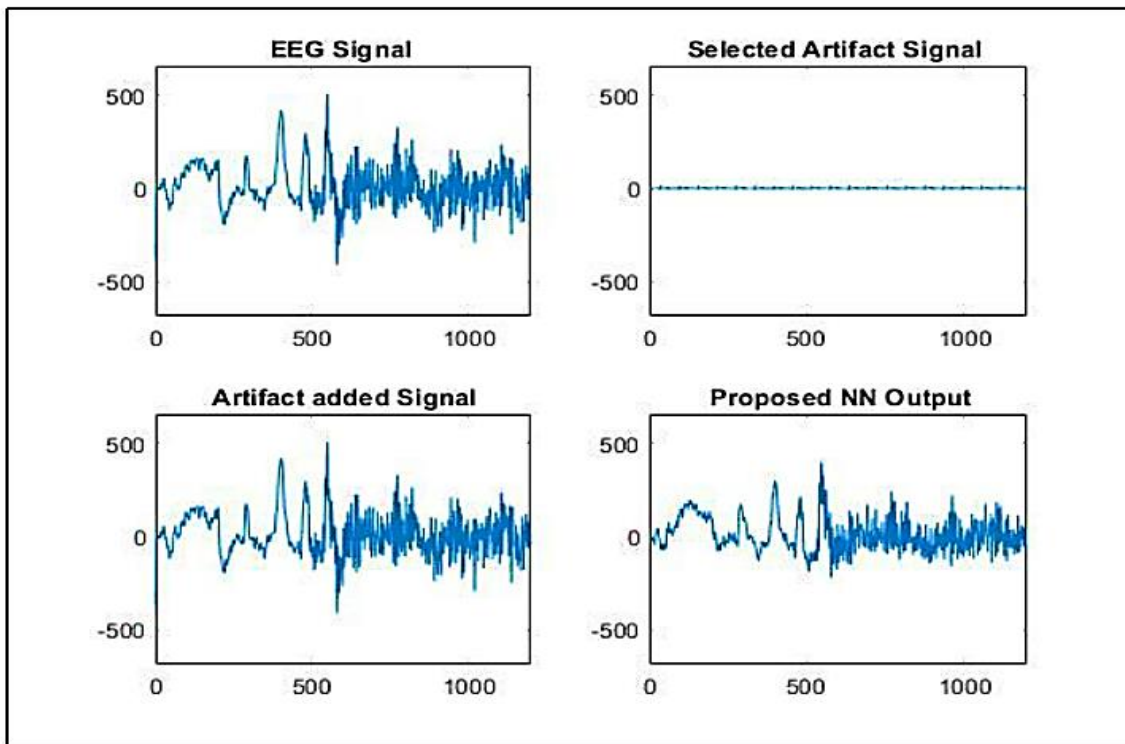


Figure 4. EEG signal with EMG artifact

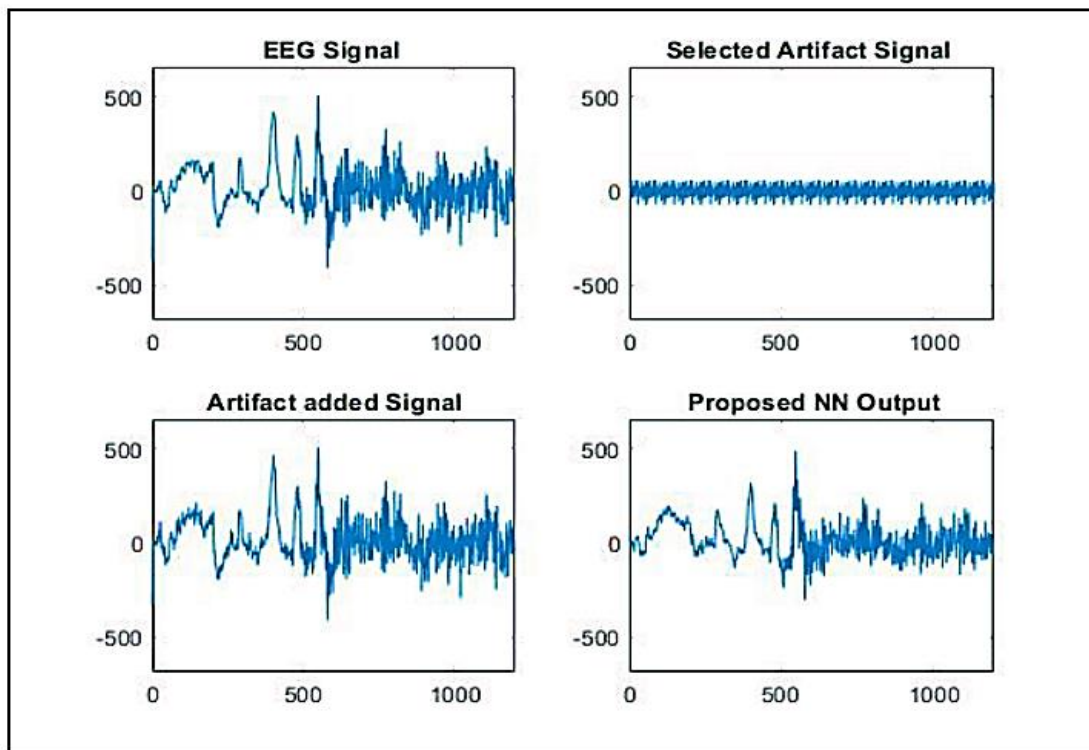


Figure 5. EEG signal with EOG artifact

In the quantitative analysis the table, I depict the error analysis of the proposed model when the number of hidden neurons is changed from 20 to 40 to 60 for ECG artefacts. Figure 5 displays this investigation under the heading "ECG artefact." Here, NNPROP with hidden neuron 20 has a high SNR of 49.98, but other hidden neurons, such as NN-PROP with hidden neuron 40 and NN-PROP with hidden neuron 60, have lower SNRs of 48.43 and 48.25, respectively.

We show the MSE analysis of ECG artefact elimination. The MSE of NN-PROP with hidden neuron 40 is quite low at 4258.48, while the corresponding values for hidden neuron 20 and 60 are 4306.98 and 4499.75 respectively as shown in Table 1. Thereafter, the model's RMSE is shown. NN-RMSE PROP's is relatively small at 0.203504326 because to the inclusion of hidden neuron 60, while the values for the other neurons are 0.222304235 and 0.220682294.

Table 1. Error analysis for ECG artifact in the EEG signal

Hidden Neurons	SNR	MSE	RMSE
20	49.98	4306.98	0.222304235
40	48.43	4258.48	0.220682294
60	48.25	4499.75	0.203504326

Table 2. Error analysis for EMG artifact in the EEG signal

Hidden Neurons	SNR	MSE	RMSE
20	49.48	3288.93	0.2196213
40	49.23	3112.57	0.219543005
60	48.84	3168.05	0.223023235

Table 3. Error analysis for EOG artifact in the EEG signal

Hidden Neurons	SNR	MSE	RMSE
20	50.42	3231.01	0.217977832
40	49.51	2923.50	0.219762968
60	49.12	3129.27	0.220123359

Table 2 presents findings from a study investigating errors arising from EMG artefact subtraction, enabling analysis through manipulated buried neurons. Results indicate that employing a variation of NN-PROP with hidden neuron 60 yields a notable SNR of 49.48. In contrast, utilizing hidden neurons 20 and 40 in other variants results in lower SNR values of 49.23 and 48.84, respectively. These outcomes highlight the impact of hidden neuron selection on SNR, emphasizing the efficacy of specific configurations in optimizing signal quality during EMG artefact removal.

The mean standard error for cleaning up EMG data is discussed. When comparing the various NN-PROP variants, it can be seen that the one with hidden neuron 40 has the lowest MSE value, at 3112.57, while the others have very high values, such as 3288.93 and 3168.05. The root-mean-square error (RMSE) analysis for cleaning up EMG signals follows. The RMSE for NN-PROP with hidden neuron 40 is 0.219543005, which is less than the RMSE for NN-PROP with hidden neuron 20 is 0.2196213 and NN-PROP with hidden neuron 60 is 0.223023235.

Table 3 displays the results of an algorithmic study of error for the purpose of gauging the efficacy of EOG artefact removal. Here, the SNR for NN-PROP with a hidden neuron of 20 is exceptionally high at 50.42, while the SNRs for the other variants are lower at 49.51 and 49.12 at hidden neurons 40 and 60 respectively.

There is an examination of MSE with respect to the EOG artefact presented. Analysis shows that NN-PROP with hidden neuron 40 achieves the lowest MSE of 2923.50 compared to the other variants' MSE values of 3231.01 and 3129.27, respectively. The root-mean-square-error (RMSE) for each possible variant is then shown. When compared to other variants, the RMSE of NN-PROP with hidden neuron 20 is found to be 0.217977832. Hidden neuron values of 40 and 60 yield RMSE values of 0.219762968 and 0.220123359, respectively.

5. CONCLUSION AND FUTURE SCOPE

Many methods for filtering out artefacts in EEG signals have been proposed and developed thanks to this study. A hybrid optimization strategy was devised to enhance multi-channel EEG data cleaning from artefact signals through NN augmented adaptive filtering. Leveraging the combination of

LM and FF methods within the NARX NN framework, the proposed hybrid optimization algorithm primarily determined ideal weights for this purpose. Implemented in MATLAB, the NN FLM method underwent testing with real-time Physionet data, featuring artefacts like electrocardiogram (ECG), electromyography (EMG), and Electrooculogram (EOG) signals across 15 channels.

This study introduces a learning-based approach for EEG artefact removal by integrating the FLM optimization method. Initially, the EEG signal undergoes processing in an adaptive filter, where established optimization techniques such as LM and FF algorithms compute optimal weights. When applied to a NN, these methods collaborate to ascertain the most effective weights for adaptive filtering, resulting in a refined system capable of filtering out artefacts from EEG data. This advancement represents a significant stride toward improving EEG signal quality and enhancing clinical analysis accuracy. Finally, the SNR, MSE, and RMSE are evaluated between the suggested method and other variants of hidden neurons.

It is necessary to assess the created models' efficacy for the removal combined ECG and EOG artefacts in Polysomnograph recordings in real time. The suggested method can be implemented in hardware and embedded with EEG recording equipment in the future.

REFERENCE

- [1] Azpúrua, M.A., Pous, M., Silva, F. (2016). Decomposition of electromagnetic interferences in the time-domain. *IEEE Transactions on Electromagnetic Compatibility*, 58(2): 385-392. <https://doi.org/10.1109/TEMC.2016.2518302>
- [2] Roy, V., Shukla, P.K., Gupta, A.K., Goel, V., Shukla, P.K., Shukla, S. (2021). Taxonomy on EEG artifacts removal methods, issues, and healthcare applications. *Journal of Organizational and End User Computing (JOEUC)*, 33(1): 19-46. <https://doi.org/10.4018/JOEUC.2021010102>
- [3] Zou, Y., Han, J., Xuan, S., Huang, S., Weng, X., Fang, D., Zeng, X. (2014). An energy-efficient design for ECG recording and R-peak detection based on wavelet transform. *IEEE Transactions on Circuits and Systems II: Express Briefs*, 62(2): 119-123. <https://doi.org/10.1109/TCSII.2014.2368619>
- [4] Kumar, K., Chebrolu, S.K., Manikandan, R., Thomas, A.K., Anusha, P.V., Bhupathi, H.P. (2024). Optimizing aensor localization and cluster performance in wireless sensor networks through Internet of Thing (IoT) and boosted weight centroid algorithm. *Journal of Intelligent Systems and Internet of Things*, 13(2): 223-230.
- [5] Harpale, V., Bairagi, V. (2021). An adaptive method for feature selection and extraction for classification of epileptic EEG signal in significant states. *Journal of King Saud University-Computer and Information Sciences*, 33(6): 668-676. <https://doi.org/10.1016/j.jksuci.2018.04.014>
- [6] Jurica, P., Struzik, Z.R., Li, J., Horiuchi, M., Hiroyama, S., Takahara, Y., Nishitomi, K., Ogawa, K., Cichocki, A. (2018). Combining behavior and EEG analysis for exploration of dynamic effects of ADHD treatment in animal models. *Journal of Neuroscience Methods*, 298: 24-32. <https://doi.org/10.1016/j.jneumeth.2018.01.002>
- [7] Liu, Y., De Vos, M., Van Huffel, S. (2015). Compressed

- sensing of multichannel EEG signals: The simultaneous cosparsity and low-rank optimization. *IEEE Transactions on Biomedical Engineering*, 62(8): 2055-2061. <https://doi.org/10.1109/TBME.2015.2411672>
- [8] Roy, V., Shukla, S. (2019). Designing efficient blind source separation methods for EEG motion artifact removal based on statistical evaluation. *Wireless Personal Communications*, 108: 1311-1327. <https://doi.org/10.1007/s11277-019-06470-3>
- [9] Piacentino, M., Beggio, G., Zordan, L., Bonanni, P. (2018). Hippocampal deep brain stimulation: Persistent seizure control after bilateral extra-cranial electrode fracture. *Neurological Sciences*, 39: 1431-1435. <https://doi.org/10.1007/s10072-018-3444-9>
- [10] Lanquart, J.P., Nardone, P., Hubain, P., Loas, G., Linkowski, P. (2018). The dichotomy between low frequency and delta waves in human sleep: A reappraisal. *Journal of Neuroscience Methods*, 293: 234-246. <https://doi.org/10.1016/j.jneumeth.2017.09.019>
- [11] Bobba, P.B., Anwar, M.H., Bhupathi, H.P., Shirisha, P., Hamza, L. (2024). Simultaneous wireless power and data transfer in different applications. *E3S Web of Conferences*, p. 01147. <https://doi.org/10.1051/e3sconf2F202455201147>
- [12] Gaskell, A.L., Hight, D.F., Winders, J., Tran, G., Defresne, A., Bonhomme, V., Raz, A., Sleight, J.W., Sanders, R.D. (2017). Frontal alpha-delta EEG does not preclude volitional response during anaesthesia: Prospective cohort study of the isolated forearm technique. *BJA: British Journal of Anaesthesia*, 119(4): 664-673. <https://doi.org/10.1093/bja/aex170>
- [13] Smith, E.E., Reznik, S.J., Stewart, J.L., Allen, J.J. (2017). Assessing and conceptualizing frontal EEG asymmetry: An updated primer on recording, processing, analyzing, and interpreting frontal alpha asymmetry. *International Journal of Psychophysiology*, 111: 98-114. <https://doi.org/10.1016/j.ijpsycho.2016.11.005>
- [14] Suman S.K., Porselvi, S., Bhagyalakshmi L., and Kumar, D. (2014). Game theoretical approach for improving throughput capacity in wireless Ad Hoc networks. In *Proceedings of International Conference on Recent Trends in Information Technology*, Chennai, India. <https://doi.org/10.1109/ICRTIT.2014.6996152>
- [15] Bono, V., Das, S., Jamal, W., Maharatna, K. (2016). Hybrid wavelet and EMD/ICA approach for artifact suppression in pervasive EEG. *Journal of Neuroscience Methods*, 267: 89-107. <https://doi.org/10.1016/j.jneumeth.2016.04.006>
- [16] Lakshmi, K.A., Surling, S.N., Sheeba, O. (2017). A novel approach for the removal of artifacts in EEG signals. In *2017 International Conference on Wireless Communications, Signal Processing and Networking (WiSPNET)*, Chennai, India, IEEE, pp. 2595-2599. <https://doi.org/10.1109/WiSPNET.2017.8300232>
- [17] Hermans, K., De Munck, J.C., Verdaasdonk, R., Boon, P., Krausz, G., Prueckl, R., Ossenblok, P. (2016). Effectiveness of reference signal-based methods for removal of EEG artifacts due to subtle movements during fMRI scanning. *IEEE Transactions on Biomedical Engineering*, 63(12): 2638-2646. <https://doi.org/10.1109/TBME.2016.2602038>
- [18] Chakravarthy, B.K., Lakshmi, G.S., Bhupathi, H.P. (2024). Review on charging methods and charging solutions for electric vehicles. *E3S Web of Conferences*, 547: 03001. <https://doi.org/10.1051/e3sconf2F202454703001>
- [19] Szentkirályi, A., Wong, K.K., Grunstein, R.R., D'Rozario, A.L., Kim, J.W. (2017). Performance of an automated algorithm to process artefacts for quantitative EEG analysis during a simultaneous driving simulator performance task. *International Journal of Psychophysiology*, 121: 12-17. <https://doi.org/10.1016/j.ijpsycho.2017.08.004>
- [20] Sujeethadevi, T., Bhagyalakshmi, L., Suman, S.K. (2019). Enhancing the performance of wireless sensor networks through clustering and joint routing with mobile sink. *International Journal of Engineering and Advanced Technology*, 8(6): 323-327. <https://www.ijeat.org/portfolio-item/E7664068519/>
- [21] Stalin, S., Roy, V., Shukla, P.K., Zaguia, A., Khan, M.M., Shukla, P.K., Jain, A. (2021). A machine learning-based big EEG data artifact detection and wavelet-based removal: An empirical approach. *Mathematical Problems in Engineering*, 2021: 1-11. <https://doi.org/10.1155/2021/2942808>
- [22] Pandraka, V.K., Tinnavelli, R.R., Kumar, R.A., Bhupathi, H.P., Gundebommu, S.L. (2024). Effect of inverter voltage levels on torque ripples of PMSM drive. *E3S Web of Conferences*, 547: 02016. https://ui.adsabs.harvard.edu/link_gateway/2024E3SWC.54702016P/doi:10.1051/e3sconf/202454702016
- [23] Suman, S.K., Shekhar, H., Mahatn, C.B., Gururaj, D., Bhagyalakshmi, L., Patra, P.S.K. (2023). Sign language interpreter. *Advances in Cognitive Science and Communications*, pp. 1021-1031. https://doi.org/10.1007/978-981-19-8086-2_96